

Luttinger liquid superlattices

This article has been downloaded from IOPscience. Please scroll down to see the full text article.

2001 J. Phys.: Condens. Matter 13 L619

(<http://iopscience.iop.org/0953-8984/13/27/102>)

View [the table of contents for this issue](#), or go to the [journal homepage](#) for more

Download details:

IP Address: 171.66.16.226

The article was downloaded on 16/05/2010 at 13:52

Please note that [terms and conditions apply](#).

LETTER TO THE EDITOR

Luttinger liquid superlattices**J Silva-Valencia¹, E Miranda¹ and Raimundo R dos Santos²**¹ Instituto de Física ‘Gleb Wataghin’, Unicamp, C.P. 6165, 13083-970 Campinas SP, Brazil² Instituto de Física, Universidade Federal do Rio de Janeiro, C.P. 68.528, 21945-970 Rio de Janeiro RJ, Brazil

Received 25 April 2001

Published 22 June 2001

Online at stacks.iop.org/JPhysCM/13/L619**Abstract**

We calculate the correlation functions and the dc conductivity of Luttinger liquid superlattices, modelled by a repeated pattern of interacting and free Luttinger liquids. In a specific realization, where the interacting subsystem is a Hubbard chain, the system exhibits a rich phase diagram with four different phases: two metals and two compressible insulators. In general, we find that the effective low-energy description amalgamates features of both types of liquids *in proportion to their spatial extent*, suggesting the interesting possibility of ‘engineered’ Luttinger liquids.

In recent years, new experimental techniques have made it possible to grow nanostructures which are topologically one-dimensional, such as quantum wires and Carbon nanotubes. However, care must be taken when invoking existing models to discuss their electronic properties, since inhomogeneities must be taken into account in a fundamental way. Consider, for instance, the Luttinger liquid (LL), which is the standard model for low-energy phenomena involving interacting electrons in one dimension [1]. The absence of conductance renormalization in long high-mobility GaAs wires [2] has been explained in terms of a usual LL (representing the wire) in contact with a non-interacting LL at each of its ends (representing the Fermi liquid leads); that is, overall, the system can be thought of as an *inhomogeneous Luttinger Liquid* (ILL). LLs with different inhomogeneity profiles have also been used in the context of the fractional quantum Hall effect (FQHE), to describe transitions between edge states at different fillings [3, 4], or between an edge state connected to a Fermi liquid [5]. A different class of inhomogeneous systems is represented by superlattices (SLs) and multilayers. By varying the relative thicknesses of the repeating unit in magnetic metallic multilayers, fascinating properties such as exchange oscillation and giant magneto-resistance (GMR) have been found [6]. The interplay between electron correlations and a SL structure (or layering) can therefore lead to collective properties quite distinct from those of each of its constituents. Furthermore, the ability to manipulate physical properties by choosing an appropriate spatial modulation opens the way for a whole new set of ‘engineered’ materials.

With this in mind, our purpose here is to discuss the properties of a one-dimensional SL made up of a periodic arrangement of two long and perfectly connected LLs, one interacting and the other free. Accordingly, the low-energy properties of this Luttinger liquid superlattice (LLSL) are described by generalizing the usual bosonized Hamiltonian [1, 7, 8] as follows,

$$H = \frac{1}{2\pi} \sum_{v=\rho,\sigma} \int dx \left\{ u_v(x) K_v(x) (\partial_x \Theta_v)^2 + \frac{u_v(x)}{K_v(x)} (\partial_x \Phi_v)^2 \right\} \quad (1)$$

where the sum extends over separated charge ($v = \rho$) and spin ($v = \sigma$) degrees of freedom, each with layer-dependent parameters $u_v(x)$ and $K_v(x)$; these determine, respectively, the velocity of elementary excitations and the algebraic decay of correlations functions for each degree of freedom. For x on the free layer one has $K_v(x) = 1$ and $u_v(x) = v_F$, the Fermi velocity, whereas for x on the repulsive layer $K_v(x)$ and $u_v(x)$ become the usual uniform LL parameters. For definiteness, we will often speak of a ‘Hubbard superlattice’ (HSL), where the interacting layer is taken as a Hubbard model with hopping t and on-site repulsion U [9, 10]; a weak coupling perturbation theory similar to that of the homogeneous model can be used to show that equation (1) indeed describes the low energy and small momentum sector of the discrete model with long layers [11]. In the homogeneous case, the dependence of the LL parameters on both the density and U has been determined by recourse to the exact solution [12–15]. With respect to magnetic properties, the SL structure does not break spin SU(2) symmetry, so that the inhomogeneous K_σ is still expected to renormalize to $K_\sigma^* = 1$. The spin sector stiffness is therefore unrenormalized as in the homogeneous system³.

The boson phase fields Φ_v are related to the charge and spin densities, ρ and σ , through $\sqrt{2}\partial_x \Phi_v(x)/\pi = \nu$, while Θ_v is such that $\partial_x \Theta_v$ is the momentum field conjugate to Φ_v : $[\Phi_v(x), \partial_y \Theta_{v'}(y)] = i\delta_{v,v'}\delta(x-y)$. Φ_v and Θ_v are dual fields, since they satisfy both

$$\partial_t \Phi_v = u_v(x) K_v(x) \partial_x \Theta_v \quad (2)$$

and the equation obtained through the replacements $\Phi_v \rightarrow \Theta_v$, $\Theta_v \rightarrow \Phi_v$, and $K_v \rightarrow 1/K_v$. These equations can be uncoupled to yield

$$\partial_{tt} \Phi_v - u_v K_v \partial_x \left(\frac{u_v}{K_v} \partial_x \Phi_v \right) = 0 \quad (3)$$

and a dual equation for Θ_v .

The equations of motion are subject to the continuity of Φ_v and Θ_v [16, 17] (which ensures the continuity of the fermionic field). Since their time derivatives are also continuous, equation (2) and its dual yield, as additional conditions, the continuity of $(u_v/K_v)\partial_x \Phi_v$ and $u_v K_v \partial_x \Theta_v$ at the contacts. Thus, both charge and spin currents $j_v = \sqrt{2}\partial_t \Phi_v/\pi$ are conserved, since we neglect Umklapp processes and spin backscattering.

The Hamiltonian (1) is straightforwardly diagonalized by a normal mode expansion

$$\Phi_v(x, t) = -i \sum_{p \neq 0} \text{sgn}(p) \frac{\phi_{p,v}(x)}{2\sqrt{\omega_{p,v}}} [b_{-p,v} e^{i\omega_{p,v}t} + b_{p,v}^\dagger e^{-i\omega_{p,v}t}] - \phi_{0,v}(x) + \gamma_{\lambda v} t \quad (4)$$

$$\Theta_v(x, t) = i \sum_{p \neq 0} \frac{\theta_{p,v}(x)}{2\sqrt{\omega_{p,v}}} [b_{-p,v} e^{i\omega_{p,v}t} - b_{p,v}^\dagger e^{-i\omega_{p,v}t}] + \theta_{0,v}(x) - \tau_{\lambda v} t \quad (5)$$

where $b_{p,v}^\dagger$ are boson creation operators ($p > 0$). $\phi_{0,v}(x)$ and $\theta_{0,v}(x)$ are the zero mode functions which, in the homogeneous case, are given by $\phi_{0,v}(x) = N_v \pi x/L$, $\theta_{0,v}(x) = J_v \pi x/L$, where N_v and J_v are the (charge and spin) number and current operators. Moreover, in this case $\gamma_v = \pi u_v K_v J_v/L$ and $\tau_v = \pi(u_v/K_v)N_v/L$. However, in a LLSL

³ However, a gap has been predicted in HSL’s with an even number of electrons on *short* repulsive layers [9, 10].

the inhomogeneity will induce a modulation of the charge (but not of the spin) density of the system. Thus, one needs to introduce, in general, *layer-specific* number and current operators. Since each layer is a LL, the variations across the layers are $\Delta\phi_{0,v} = \pi N_{\lambda v}$ and $\Delta\theta_{0,v} = \pi J_{\lambda v}$, where $\lambda = 0$ or U , depending on whether the layer is free or interacting, respectively. $\phi_{0,v}(x)$ and $\theta_{0,v}(x)$ will then be linear continuous functions of x , with slopes given by the layer number and current operators (we omit the expressions for brevity). Analogously, from the equations of motion (2), we obtain $\gamma_{\lambda v}$ and $\tau_{\lambda v}$.

In order to find the equilibrium value of the density in each layer, one needs to equate their chemical potentials

$$\mu_0(n_0) = \mu_0(n + \ell(n - n_U)) = \mu_U(n_U) \quad (6)$$

where $n = N/L$ is the total electron density, $\ell = L_U/L_0$ and μ_λ and n_λ are the chemical potential and density of each layer, respectively. For definiteness, we have determined the charge profile in a HSL using the exact expression for $\mu_U(n_U)$ [13]. We found that the charge tends to accumulate in the free layer. This is rather intuitive, since electrons decrease their mutual repulsion energy by flowing into the free layer. This was observed in numerical studies of the HSL [10]. Of course, such a charge inhomogeneity will be strongly suppressed with the inclusion of long-range Coulomb interactions, which are absent in a Hubbard model description.

The HSL has a very rich phase diagram. For $n < 1$ the system is always metallic. For $n > 1$, however, we observe four different phases, two metallic and two insulating, each characterized by its charge profile, as shown in figure 1. The two insulating phases correspond to either $n_U = 1$ (Mott insulator) or $n_0 = 2$ (band insulator). Note that, in each case, one type of layer is by itself insulating while the other is metallic, the overall insulating character being a consequence of the 1D structure ('resistors in series'). Therefore, both insulating phases are *gapless*, except at the phase boundary indicated by the dashed line in figure 1, where *both* $n_U = 1$ and $n_0 = 2$ and the system exhibits a Mott–Hubbard gap. The density at this line is thus $n_c = (2 + \ell)/(1 + \ell)$ [18]. The two metallic phases differ in the density of the interacting layer: the chemical potential can fall in either its upper or its lower Hubbard band. For values of $U > U_c \approx 3.2309t$, the system cannot sustain the upper metallic phase. This value is independent of the 'aspect ratio' ℓ . Note that, for $U < U_c$, the HSL is always gapless.

While the topology of the phase diagram of figure 1 is specific to a HSL, we expect that several of its features should be generic to other LLSLs. In particular, the 'division of labour' between the two subsystems, where one is responsible for the insulating behaviour whereas the other renders the system compressible, is reflected in the weighted form of the SL compressibility

$$\kappa_s = \frac{1}{L} \left(\frac{\partial^2 E_0}{\partial N^2} \right)^{-1} = \frac{\kappa_0 + \ell\kappa_U}{1 + \ell} \quad (7)$$

where $\kappa_U = 2K_\rho/\pi u_\rho$ and $\kappa_0 = 2/\pi v_F$ are the compressibilities of the interacting and free layers respectively.

The SL structure also affects the velocity of excitations. For $p \ll \pi/(L_U + L_0)$, the dispersion relation of the LLSL is linear, with effective velocities

$$c_v = \frac{v_F(1 + \ell)}{\sqrt{1 + \Delta_v \ell v_F/u_v + (\ell v_F/u_v)^2}} \quad (8)$$

where $\Delta_v = K_v + K_v^{-1}$. Clearly, $c_v \rightarrow u_v$ as $\ell \rightarrow \infty$, and $c_v \rightarrow v_F$ as $\ell \rightarrow 0$. Furthermore, as one approaches the insulating phase from the low-density region (see figure 1), $c_\rho \rightarrow 0$ as a result of $u_\rho \rightarrow 0$ in the interacting layer. As in the homogeneous system, the LL description

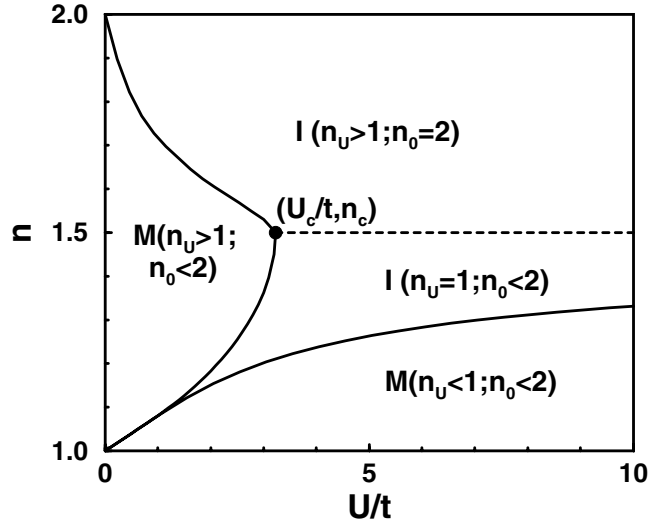


Figure 1. Phase diagram of a Hubbard superlattice showing two metallic (M) and two insulating (I) phases ($\ell = 1$) ($U_c/t \approx 3.2309$ and $n_c = (2 + \ell)/(1 + \ell)$).

breaks down whenever a gap opens in the charge or spin sector of either layer. In the HSL case, this happens in both insulating regions of figure 1. Note, however, that the determination of the phases through equation (6) does not rely on the LL description.

We now focus on the correlations. The $T = 0$ asymptotic behaviour (i.e. for well separated x and y) of charge and spin correlations is given by

$$\langle n(x)n(y) \rangle \sim \frac{\alpha_\rho}{\pi^2|x-y|^2} + A_1 \frac{e^{2i(\bar{\phi}_0(y)-\bar{\phi}_0(x))}}{|x-y|^{1+K_\rho^*}} + A_2 \frac{e^{4i(\bar{\phi}_0(y)-\bar{\phi}_0(x))}}{|x-y|^{4K_\rho^*}} \quad (9)$$

$$\langle \mathbf{S}(x) \cdot \mathbf{S}(y) \rangle \sim \frac{\alpha_\sigma}{\pi^2|x-y|^2} + B_1 \frac{e^{2i(\bar{\phi}_0(y)-\bar{\phi}_0(x))}}{|x-y|^{1+K_\rho^*}} \quad (10)$$

where $\bar{\phi}_0(x) = k_F x - \phi_{0,\rho}(x)$ and the LLSL effective exponent is

$$K_\rho^* = \frac{\sqrt{1 + \Delta_\rho \ell v_F / u_\rho + (\ell v_F / u_\rho)^2}}{1 + \ell v_F / K_\rho u_\rho} \equiv f(K_\rho) \quad (11)$$

where α_ν is a function of system parameters and the layer. Similarly, correlation functions for singlet and triplet superconducting pairings are

$$\langle O^\dagger(x)O(y) \rangle \sim \frac{C}{|x-y|^{1+\bar{K}_\rho}} \quad (12)$$

where $\bar{K}_\rho = f(1/K_\rho)$. One should note that the correlation functions depend not only on the difference $x - y$, but also on the actual positions x and y , through the zero mode functions. Their effect will be to generate the usual spatial oscillations present in homogeneous LLs. However, due to the inhomogeneous density profile, their period will vary from layer to layer, reflecting the layer-dependent Fermi wavevectors; this is akin to the oscillatory behaviour of the exchange coupling in magnetic metallic multilayers [6, 10]. In spite of the presence of effective exponents K_ρ^* and \bar{K}_ρ , the condition for dominant superconducting correlations reduces to the one for homogeneous systems, namely $K_\rho > 1$. The dominant term in the charge and spin correlation functions is the second one, which in the homogeneous case corresponds to the

$2k_F$ contribution. This predominance, however, may be superseded by the behaviour of the amplitude A_1 , as discussed in [19].

In figure 2, the correlation exponent K_ρ^* of a HSL is shown as a function of filling, for $\ell = 1$. Both metallic phases are characterized by $1/2 < K_\rho^* < 1$. On the low-density side, K_ρ^* approaches a value larger than $1/2$ as $n \rightarrow 0$, which depends on ℓ but not on U . This is a feature unique to the LLSL. Note from equation (11) that K_ρ^* interpolates monotonically between 1 (the free value) and K_ρ (the interacting layer exponent) as ℓ is varied from 0 to ∞ . This illustrates a general feature of the LLSL, namely by varying the ‘aspect ratio’ ℓ , one can fine-tune a physical property to a specified value.

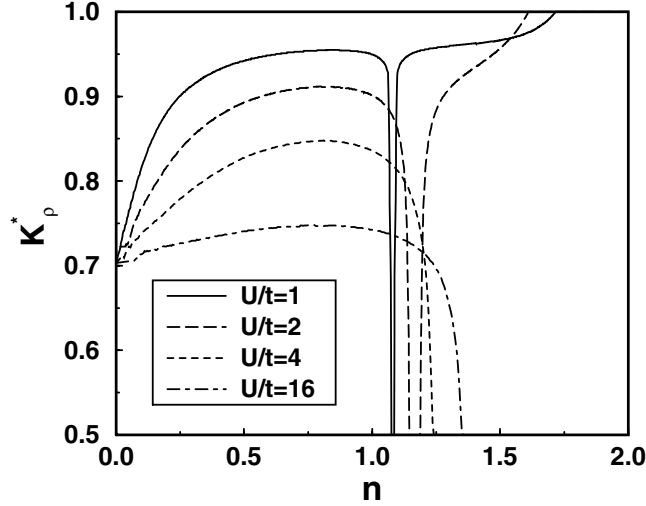


Figure 2. The correlation exponent K_ρ^* of a Hubbard superlattice as a function of the total electron density n for $\ell = 1$ and different values of U .

Finally, we discuss the transport properties of a LLSL. In the presence of an applied electric field the equation of motion for Φ_ρ becomes [16, 17]

$$\left[-\frac{\partial_{tt}}{u_\rho K_\rho} + \partial_x \left(\frac{u_\rho}{K_\rho} \partial_x \right) \right] \Phi_\rho(x, t) = -eE(x, t). \quad (13)$$

The non-local conductivity is given by

$$\sigma(x, y, t) = -\frac{2g_o}{\pi} \partial_t G(x, y, t) \quad (14)$$

where $g_o = e^2/h$ is the conductance quantum and $G(x, y, t) = -i\theta(t)\langle [\Phi_\rho(x, t), \Phi_\rho(y, 0)] \rangle$ is the bosonic Green's function.

We first calculate the Drude conductivity, which gives the current response to a uniform electric field: $\lim_{\omega \rightarrow 0} \sigma(q = 0, \omega)$ [20]. A straightforward calculation yields

$$\sigma(q = 0, \omega) = 2g_o c_\rho K_\rho^* \delta(\omega). \quad (15)$$

The delta function coefficient is the Drude weight. It has the same form as for the homogeneous case [12], but with the effective velocity and effective exponent replacing the corresponding uniform quantities u_ρ and K_ρ . By plugging in the results from equations (8) and (11), one recognizes the conductivity of resistors connected in series.

We have plotted the Drude weight of a HSL as a function of n for $\ell = 1$ and several values of U in figure 3. The plot shows the re-entrant behaviour as a function of n for $U < U_c$.

Furthermore, the Drude weight dips to zero upon approaching the insulating regions as a result of the vanishing charge velocities $u_\rho \rightarrow 0$ (Mott insulator) and $v_F \rightarrow 0$ (band insulator).

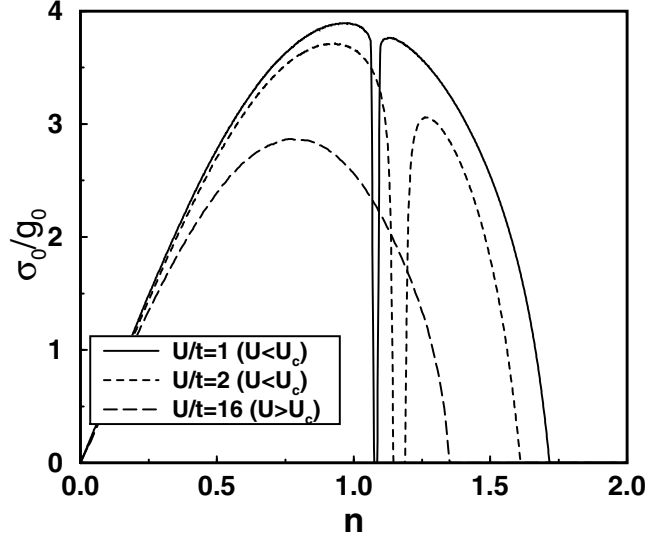


Figure 3. The Drude weight of a Hubbard superlattice as a function of n for $\ell = 1$ and different values of U .

A more common experimental situation occurs when a field is applied to a finite region of the sample. In this case, the inverse order of limits applies $\lim_{q \rightarrow 0} \sigma(q, \omega = 0)$, and we obtain the Landauer conductance [20]. In the LLSL

$$\sigma(q, \omega = 0) = 2g_o K_\rho^* \delta(q). \quad (16)$$

Once again, the result is in close analogy with the homogeneous system [21], where the SL interaction exponent has replaced the homogeneous one. Both Drude and Landauer responses, therefore, can be modulated by changing the SL spacing. However, the interaction renormalization of equation (16) is not revealed in usual dc conductance measurements, where it is masked by the presence of the Fermi liquid leads [16]. In a LLSL of length L , only by going to frequencies of the order of the inverse traversal time $\omega > u_\rho/L$ can the influence of the K_ρ^* exponent be felt [22].

In closing, we would like to highlight the fact that the low-energy, long-wavelength properties of a LLSL can be, in effect, subsumed into a few effective parameters, in close analogy with the usual homogeneous LL description. These effective parameters, on the other hand, turn out to be weighted averages of the underlying subsystem properties, in rough proportion to their spatial extent (see, e.g., equations (7), (8) and (11)). Such a ‘tempered Luttinger liquid’ description suggests the interesting possibility of creating SL structures with properties engineered to suit a particular purpose, in a way reminiscent of modulation-doped semiconductor heterostructures and magnetic multilayers. Whether this will prove feasible, however, remains to be seen.

In summary, we have considered Luttinger liquid superlattices made up of a periodic arrangement of free and repulsive Luttinger liquids. Due to the space-dependent properties of the system, a non-homogeneous charge profile ensues. A specific realization of such a system, a Hubbard superlattice, was investigated in detail and its phase diagram was shown to exhibit two metallic phases and two peculiar compressible insulating ones.

The authors are grateful to A O Caldeira and T Paiva for discussions. Financial support from the Brazilian Agencies CNPq, FAPESP (E.M.), and FAPERJ (R.R.d.S.) is also gratefully acknowledged.

References

- [1] Voit J 1994 *Rep. Prog. Phys.* **57** 977
- [2] Tarucha S, Honda T and Saku T 1995 *Solid State Commun.* **94** 413
- [3] Oreg Y and Finkel'stein A M 1993 *Phys. Rev. Lett.* **74** 3668
- [4] Chklovskii D B and Halperin B 1998 *Phys. Rev. B* **57** 3781
- [5] de C Chamon C and Fradkin E 1997 *Phys. Rev. B* **56** 2012
- [6] Baibich M N and Muniz R B 1992 *Brazil. J. Phys.* **22** 253
Heinrich B and Cochran J F 1993 *Adv. Phys.* **42** 523
Hathaway K B 1994 *Ultrathin Magnetic Structures* vol II, ed B Heinrich and J A C Bland (Berlin: Springer)
- [7] Emery V J 1979 *Highly Conducting One-dimensional Solids* ed J T Devreese, R P Evrard and V E Van Doren (New York: Plenum) p 247
- [8] Haldane F D M 1981 *J. Phys. C: Solid State Phys.* **14** 2585
- [9] Paiva T and dos Santos R R 1996 *Phys. Rev. Lett.* **76** 1126
- [10] Paiva T and dos Santos R R 2000 *Phys. Rev. B* **62** 7007
- [11] Safi I 1997 *Ann. Phys., Paris* **22** 463
- [12] Schulz H J 1990 *Phys. Rev. Lett.* **64** 2831
Schulz J 1991 *Int. J. Mod. Phys. B* **5** 57
- [13] Lieb E H and Wu F Y 1968 *Phys. Rev. Lett.* **20** 1445
- [14] Frahm H and Korepin V E 1990 *Phys. Rev. B* **42** 10 553
- [15] Kawakami N and Yang S K 1990 *Phys. Lett. A* **148** 359
- [16] Safi I and Schulz H J 1995 *Phys. Rev. B* **52** R17040
Maslov D L and Stone M 1995 *Phys. Rev. B* **52** R5539
Ponomarenko V V 1995 *Phys. Rev. B* **52** R8666
- [17] Safi I and Schulz H J 1999 *Phys. Rev. B* **59** 3040
- [18] Paiva T and dos Santos R R 1998 *Phys. Rev. B* **58** 9607
- [19] Paiva T and dos Santos R R 2000 *Phys. Rev. B* **61** 13 480
- [20] Fenton E W 1992 *Phys. Rev. B* **46** 3754
- [21] Apel W and Rice T M 1982 *Phys. Rev. B* **26** 7063
- [22] Matveev K A and Glazman L I 1993 *Physica B* **189** 266